Higher-order figure-8 microphones/hydrophones collocated as a perpendicular triad—Their "spatial-matched-filter" beam steering

Shiyu Sandy Du, Kainam Thomas Wong, Yang Song, et al.

Citation: The Journal of the Acoustical Society of America **151**, 1158 (2022); doi: 10.1121/10.0009312
View online: https://doi.org/10.1121/10.0009312
View Table of Contents: https://asa.scitation.org/toc/jas/151/2
Published by the Acoustical Society of America

JASA ARTICLE

Higher-order figure-8 microphones/hydrophones collocated as a perpendicular triad—Their "spatial-matched-filter" beam steering

Shiyu Sandy Du,[1] Kainam Thomas Wong,[1,a)] Yang Song,[2] Chibuzo Joseph Nnonyelu,[3] and Yue Ivan Wu[4]
[1]*School of General Engineering, Beihang University, Beijing, 100191, China*
[2]*School of Electrical and Electronic Engineering, Nanyang Technological University, 639798, Singapore*
[3]*Sensible Things that Communicate Research Centre, Mid Sweden University, Sundsvall, Sweden*
[4]*College of Computer Science, Sichuan University, Chengdu, Sichuan, 610065, China*

ABSTRACT:
Directional sensors, if collocated but perpendicularly oriented among themselves, would facilitate signal processing to uncouple the azimuth-polar direction from the time-frequency dimension—in addition to the physical advantage of spatial compactness. One such acoustical sensing unit is the well-known "tri-axial velocity sensor" (also known as the "gradient sensor," the "velocity-sensor triad," the "acoustic vector sensor," and the "vector hydrophone"), which comprises three identical figure-8 sensors of the *first* directivity-order, collocated spatially but oriented perpendicularly of each other. The directivity of the figure-8 sensors is hypothetically raised to a *higher* order in this analytical investigation with an innocent hope to sharpen the overall triad's directionality and steerability. Against this wishful aspiration, this paper rigorously analyzes how the directivity-order would affect the triad's "spatial-matched-filter" beam's directional steering capability, revealing which directivity-order(s) would allow the beam-pattern of full maneuverability toward any azimuthal direction and which directivity-order(s) cannot.
 https://doi.org/10.1121/10.0009312
(Received 30 August 2021; revised 28 November 2021; accepted 23 December 2021; published online 18 February 2022)
[Editor: Mingsian R. Bai] Pages: 1158–1170

I. INTRODUCTION

A. "Figure-8" directional microphones/hydrophones

One common directional microphone/hydrophone is the figure-8 sensor, which has a dipole-like directional response of $\cos^k(\gamma)$, where $k \in \{1, 2, \ldots\}$ symbolizes the sensor's directivity-order, and $\gamma \in [0, 2\pi)$ denotes the incident source's incident angle with respect to the sensor axis.

This $\cos^k(\gamma)$ gain response graphically resembles the digit "8," hence, the figure-8 label. As the directivity-order k increases, the figure-8 sensor's gain pattern narrows, providing greater sensitivity toward an incident direction that is more parallel to the sensor's axis. Please refer to Fig. 1.

Concerning the higher-order directional microphones/hydrophones, their directivity and beam-patterns have been investigated in Refs. 1–12, whereas azimuth-elevation direction-of-arrival formulas are devised for them in Ref. 13.

For further discussions of higher-order figure-8 sensors, please consult Chap. 8.3 and 8.5 of Ref. 14 and Chap. 2 of Ref. 15.[13,16]

B. A triad of figure-8 sensors in orthogonal orientation and spatial collocation

Place three figure-8 sensors at the origin of the Cartesian coordinates and orient one each along the x, y, and z axes. Such a collocated perpendicular triad has a 3×1 array manifold[17–19] of

$$\mathbf{a}_k(\theta, \phi) = \begin{bmatrix} \{\sin(\theta)\cos(\phi)\}^k \\ \{\sin(\theta)\sin(\phi)\}^k \\ \{\cos(\theta)\}^k \end{bmatrix} \tag{1}$$

$$\equiv \mathbf{a}_k(\theta, \phi) = \begin{bmatrix} u^k(\theta, \phi) \\ v^k(\theta, \phi) \\ w^k(\theta) \end{bmatrix}, \tag{2}$$

where $\theta \in [0, \pi]$ symbolizes the incident acoustic wave's polar direction-of-arrival (also known as the zenith angle), $\phi \in [0, 2\pi)$ signifies the associated azimuth direction-of-arrival, whereas $u(\theta, \phi) \stackrel{\text{def}}{=} \sin(\theta)\cos(\phi)$, $v(\theta, \phi) \stackrel{\text{def}}{=} \sin(\theta)\sin(\phi)$, and $w(\theta) \stackrel{\text{def}}{=} \cos(\theta)$, respectively, denote the Cartesian direction cosines along the x, y, and z axes. The subsequent analysis will abbreviate $u(\theta, \phi)$ as u, $v(\theta, \phi)$ as v, and $w(\theta)$ as w.[20]

The above array manifold in Eqs. (1) and (2) at any natural number k is bivariate in terms of the polar-azimuthal bivariate coordinates of (θ, ϕ), although the triad is point-like compact in spatial geometry.

Also important is the above array manifold's independence of the frequency and emitter/sensor distance (regardless

a)Electronic mail: ktwong@ieee.org, ORCID: 0000-0002-1583-6682.

https://doi.org/10.1121/10.0009312

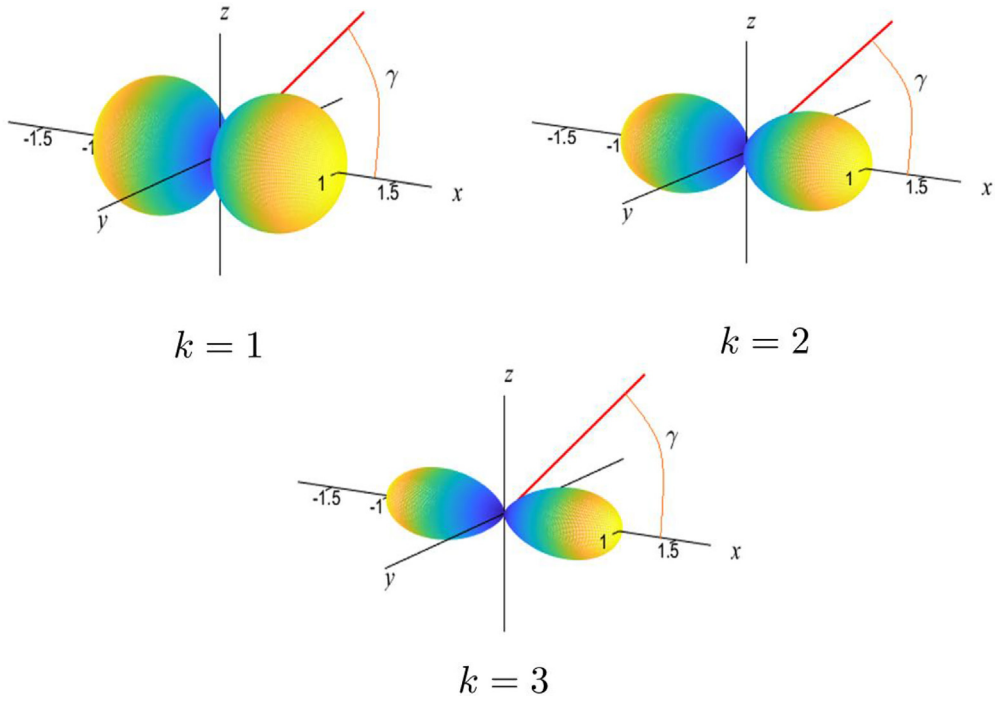

FIG. 1. (Color online) The figure-8 sensor's gain response at various directivity-orders of k.

of k). That is, the three component-sensors' spatial collocation intrinsically decouples the data's time-frequency dimensions from the data's azimuth-elevation-radial spatial dimensions.

C. The triad's spatial-matched-filter beam-pattern

The "spatial-matched-filter" (SMF) beamformer[21] (also known as "fixed beamforming" or "conventional beamforming") is a data-independent but steerable beamformer. For a "look direction" of interest $(\theta_{\text{look}}, \phi_{\text{look}})$, the SMF beamformer's weight-vector $\mathbf{w}$ (by definition) is preset to match that desired direction's nominal steering vector $\mathbf{w} = \mathbf{a}(\theta_{\text{look}}, \phi_{\text{look}})$. This beamformer is "fixed" as its beamforming weights in $\mathbf{w}$ are pre-established prior to any empirical measurement and, hence, independent of any data received. This beamforming method is "conventional" in that it predates more complicated beamforming algorithms that adapt to the signal/interference/noise information embedded in the received data. In the case in which the interference and additive noise may, together, be modeled statistically as (1) zero-mean, (2) spatially uncorrelated, and (3) uncorrelated with the desired signal, the SMF output's signal-to-noise ratio (SNR) is maximum relative to any other beamformer's output.

Consider the figure-8 sensor triad of Eqs. (1) and (2). This triad's SMF beamformer, preset to a look direction of $(\theta, \phi) = (\theta_{\text{look}}, \phi_{\text{look}})$, would have an amplitude beam-pattern of

$$B_k^{(\theta_{\text{look}},\phi_{\text{look}})}(\theta,\phi) \stackrel{\text{def}}{=} [\mathbf{a}_k(\theta_{\text{look}},\phi_{\text{look}})]^T \mathbf{a}_k(\theta,\phi), \tag{3}$$

or in terms of the Cartesian direction cosines as

$$B_k^{(u_{\text{look}},v_{\text{look}},w_{\text{look}})}(u,v,w) = u_{\text{look}}^k u^k + v_{\text{look}}^k v^k + w_{\text{look}}^k w^k. \tag{4}$$

In Eq. (3), the superscript ^{T} denotes transposition. Furthermore, $u_{\text{look}} \stackrel{\text{def}}{=} u(\theta_{\text{look}}, \phi_{\text{look}})$, $v_{\text{look}} \stackrel{\text{def}}{=} v(\theta_{\text{look}}, \phi_{\text{look}})$, and $w_{\text{look}} \stackrel{\text{def}}{=} w(\theta_{\text{look}})$.

The above beam-pattern for the *first*-order case of $k = 1$ has been analyzed previously in Refs. 22–26, but those references are unconcerned with the *higher*-order figure-8 sensors (where $k \geq 2$, as in this present work). For *higher*-order figure-8 sensors collocated in orthogonality, their SMF beam-pattern has been investigated: in Ref. 27, which concerns the triad's beam-pattern's general features but not about the pointing bias, and Ref. 28 for a *pair* but not for a triad as in this work.

This paper will be first in the open literature to investigate the beam steering capability of a tri-axial collocated unit of perpendicular *higher*-order figure-8 sensors. That is, given

(i) the sensor hardware's directivity-order of k, and
(ii) the beamforming software's algorithmic setting of the desired look direction of $(\theta_{\text{look}}, \phi_{\text{look}})$,

can the beam-pattern magnitude's actual peak direction,

$$(\theta_{\text{act}}, \phi_{\text{act}}) \stackrel{\text{def}}{=} \stackrel{\arg\max}{\forall(\theta,\phi)} |B_k^{(\theta_{\text{look}},\phi_{\text{look}})}(\theta,\phi)|, \tag{5}$$

be electronically steered to any polar-azimuthal direction in $\{\theta_{\text{look}} \in [0,\pi]\} \cup \{\phi_{\text{look}} \in [0,2\pi)\}$? Here, the SMF beamformer's actual peak $(\theta_{\text{act}}, \phi_{\text{act}})$, by definition, is the direction where the beam output's *magnitude* $|B_k^{(\theta_{\text{look}},\phi_{\text{look}})}(\theta,\phi)|$ is largest. If the answer is "yes" to the above question, will

$(\theta_{act}, \phi_{act}) = (\theta_{look}, \phi_{look})$? That is, will no steering bias exist? These questions' answers will be uncovered in this paper as "yes," but, unexpectedly, if and only if $k = 1$.

Although this beamformer output $B_k^{(\theta_{look},\phi_{look})}(\theta, \phi)$ equals the inner product of the two vectors of $\mathbf{a}_k(\theta_{look}, \phi_{look})$ and $\mathbf{a}_k(\theta, \phi)$, setting $(\theta, \phi) = (\theta_{look}, \phi_{look})$ will render the two vectors parallel but will *not* necessarily maximize $|B_k^{(\theta_{look},\phi_{look})}(\theta, \phi)|$. This is because the array manifold $\mathbf{a}_k(\theta, \phi)$ of Eq. (1) has a second norm (i.e., a vectorial length), which varies with (θ, ϕ), $\forall k \geq 2$. The right side of (4) equals the cosine of the angle between $(u_{look}, v_{look}, w_{look})$ and (u, v, w) regardless of $(u_{look}, v_{look}, w_{look})$ and (u, v, w) only if $k = 1$. Indeed, this variable-norm complication, intrinsic in the array manifold $\mathbf{a}_k(\theta, \phi)$ of Eq. (1), requires this paper's meticulous derivation to determine the beam-pointing error.

D. The organization of this paper

The beam-pattern in Eq. (4) looks compact, but its peak-direction analysis is complicated due to the directional periodicity in its several trigonometric functions, which are further obscured by being raised to a power of k.

The beam-pattern's following symmetry properties will nonetheless simplify the subsequent analysis:

(a) For any odd $k \geq 1$,

$$|B_k^{(u_{look},v_{look},w_{look})}(u, v, w)| = |B_k^{(u_{look},v_{look},w_{look})}(-u, -v, -w)|. \quad (6)$$

(b) For any even $k \geq 2$,

$$|B_k^{(u_{look},v_{look},w_{look})}(u, v, w)| = |B_k^{(u_{look},v_{look},w_{look})}(\pm u, \pm v, \pm w)|. \quad (7)$$

The directivity-order's oddness-versus-evenness would significantly affect the subsequent derivation of the beam-pattern's global maximum: For any odd k, $B_k^{(\theta_{look},\phi_{look})}(\theta, \phi)$ could become negative (thereby a locally *minimum* amplitude represents a locally *maximum* magnitude), implying a necessity to consider both the maxima and minima of Eqs. (3) and (4) to identify the beam magnitude's peak direction. In contrast, for any even k, $0 \leq B_k^{(\theta_{look},\phi_{look})}(\theta, \phi) = |B_k^{(\theta_{look},\phi_{look})}(\theta, \phi)|$. Therefore, the subsequent analysis will investigate different directivity-orders in separate sections. Figure 2 summarizes how these various cases of directivity-orders are dealt with subsequently in the rest of this paper. All of the sub-sub-cases in Fig. 2 admittedly make arduous reading, but that multiplicity reflects the present problem's intrinsic complexity—a complexity exhaustively and detailedly tackled in the various sections to follow.

The beam-pattern $B_k^{(\theta_{look},\phi_{look})}(\theta, \phi)$ is a bivariate function of (θ, ϕ) for any hardware-implemented k and algorithmically tuned $(\theta_{look}, \phi_{look})$. To locate this bivariate function's peak on the (θ, ϕ) support region, the standard analytical procedural steps are

(1) locate (e.g., through the *method of Lagrange multiplier*) the beam's critical points (θ_c, ϕ_c);
(2) among all critical points in (1), check which are local maxima; and
(3) among all local maxima, identify the global maximum (e.g., by comparing all local maxima's beam heights).

This derivation can sometimes be easier using the parameterization in Eq. (4) in terms of the three Cartesian direction cosines (u,v,w) instead of the parameterization in Eq. (3) in terms of the spherical coordinates (θ, ϕ). The reason is twofold:

(a) The (θ, ϕ) domain would involve powers of products of the trigonometric functions, of which the first partial derivatives and the second partial derivatives need be taken, to locate the beam output's critical points and local maxima. Instead, the (u,v,w) domain involves only the polynomials in u, v, and w but no trigonometric functions, thereby simplifying the subsequent analysis despite having one more parameter.
(b) The (u,v,w) parameterization reflects the spatial symmetry of the orthogonal triad, which is that the triad remains the same regardless of any permutation of x, y, and z in the Cartesian coordinates of (x,y,z), thereby collapsing several sub-cases of (θ, ϕ) into one representative case.

Figure 2 highlights how the analysis for each directivity-order progresses through the above listed (1)–(3), sometimes skipping over certain immediate steps for reasons to be detailed in the subsequent sections. The second column in Fig. 2 is elaborated in Fig. 3.

Section II will focus on the *first*-order figure-8 sensors (i.e., $k = 1$), whose mathematical simplicity allows a direct application of differentiation to locate the peak directions. Section III will concentrate on the *second*-order figure-8 sensors (i.e., $k = 2$), using the *method of Lagrange multiplier* to locate the beam-pattern's critical points, which turn out to be only six in number, plus possibly a circular rim where the whole rim is coetaneous. These six critical points' respective beam magnitudes will be derived for comparison with each other to flag the tallest as the peak direction. Sections IV–VI will analyze every *higher* order (i.e., $\forall k \geq 3$). Their critical points will be analytically shown in Sec. IV to include all six in Sec. III for $k = 2$, plus the additional critical points (which will subsequently be proved in Sec. V as not local minima). Section VI will then identify the actual peak direction(s). Section VII will conclude the entire investigation. Please see Fig. 2 for the logical flow of Secs. II–VI.

II. THE *FIRST*-ORDER TRIAD'S PEAK DIRECTION

This section will analytically prove that at $k = 1$, the triad beam-pattern's actual peak direction $(\theta_{act}, \phi_{act})$, defined in Eq. (5), always corresponds to the nominal look direction $(\theta_{look}, \phi_{look})$.

To prove the above, first, all of the critical points $\{(\theta_c, \phi_c)\}$ are to be located by applying the "first-order partial derivative test" to Eq. (3):

https://doi.org/10.1121/10.0009312

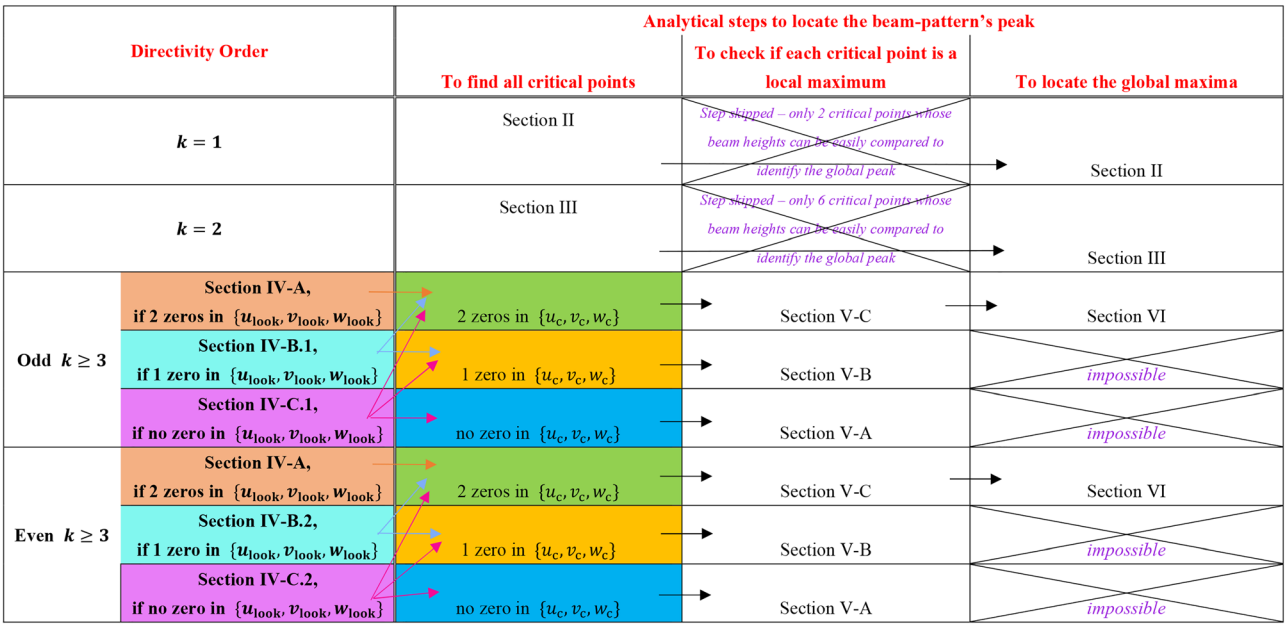

FIG. 2. (Color online) An overview of the entire paper's logical structure and logical flow. The second column here is elaborated on in the subsequent Fig. 3, where the same color is used.

(1) Set to zero:

$$\frac{\partial}{\partial\phi}B_1^{(\theta_{\text{look}},\phi_{\text{look}})}(\theta,\phi) = -\sin(\theta_{\text{look}})\cos(\phi_{\text{look}})\sin(\theta)\sin(\phi) + \sin(\theta_{\text{look}})\sin(\phi_{\text{look}})\sin(\theta)\cos(\phi),$$

thereby obtaining $\tan(\phi_c) = \tan(\phi_{\text{look}})$, which is mathematically equivalent to

$$\phi_c \in \{\phi_{\text{look}} + n\pi, \text{ for } n = 0, 1\}. \tag{8}$$

(2) Set to zero:

$$\frac{\partial}{\partial\theta}B_1^{(\theta_{\text{look}},\phi_{\text{look}})}(\theta,\phi) = \sin(\theta_{\text{look}})\cos(\phi_{\text{look}})\cos(\phi)\cos(\theta) + \sin(\theta_{\text{look}})\sin(\phi_{\text{look}})\sin(\phi)\cos(\theta) - \cos(\theta_{\text{look}})\sin(\theta). \tag{9}$$

Substitute Eq. (8) in Eq. (9) and then simplify to yield

$$0 = \sin\left(\theta_{\text{look}} - (-1)^n\theta_c\right) \leftrightarrow \theta_c \in \left\{(-1)^n\theta_{\text{look}}, (-1)^n[\theta_{\text{look}} - \pi]\right\}. \tag{10}$$

The value of n in Eq. (10) is the same as the n in Eq. (8). The first-order partial derivative test appears to give four critical points (θ_c, ϕ_c): $(\theta_{\text{look}}, \phi_{\text{look}})$, $(\theta_{\text{look}} - \pi, \phi_{\text{look}})$, $(-\theta_{\text{look}}, \pi + \phi_{\text{look}})$, and $(\pi - \theta_{\text{look}}, \pi + \phi_{\text{look}})$. However, the second point is invalid as $\theta_{\text{look}} - \pi \notin [0, \pi]$, and the third point is also invalid as $-\theta_{\text{look}} \notin [0, \pi]$. Therefore, exactly only two critical points exist,

$$(\theta_{c_1}, \phi_{c_1}) = (\theta_{\text{look}}, \phi_{\text{look}}), \quad (\theta_{c_2}, \phi_{c_2}) = (\pi - \theta_{\text{look}}, \pi + \phi_{\text{look}}). \tag{11}$$

These two directions are diametrically opposite of each other but both give a unity peak height, i.e., $B_1^{(\theta_{\text{look}},\phi_{\text{look}})}(\theta_{c_1}, \phi_{c_1}) = 1$ and $B_1^{(\theta_{\text{look}},\phi_{\text{look}})}(\theta_{c_1}, \phi_{c_1}) = -1$, $\forall(\theta_{\text{look}}, \phi_{\text{look}})$. So, both must be *global* maxima, i.e., the actual peak directions.

Consequentially, the first-order triad's beam-pattern has exactly two peaks at equal height with one peak pointing toward the nominal look direction $(\theta_{\text{act}}, \phi_{\text{act}}) = (\theta_{\text{look}}, \phi_{\text{look}})$ and the other peak pointing toward its diametrically opposite direction as specified in Eq. (11); therefore, the first-order triad's beam-pattern is bidirectional, yet, suffers *no* pointing error in the sense that the beam does peak at the nominal look direction. This conclusion concurs with

(a) the third line below Eq. (8) of Ref. 22,
(b) point (iii) in Sec. III A of Ref. 23,
(c) Eq. (10) at $\alpha = 0$ and Sec. III E of Ref. 24,
(d) Eqs. (17) and (18) in Ref. 25 with $\phi_x = \phi_y = \theta_x = \theta_y = 0$ therein,
(e) Eqs. (8) and (9) of Ref. 29, and
(f) Eqs. (17) and (18) in Ref. 26 with $\phi_{\text{mis}} = \theta_{\text{mis}} = 0$ therein.

III. THE *SECOND*-ORDER FIGURE-8 TRIAD'S PEAK DIRECTION

For the directivity-order $k = 2$, this section will analytically prove that the beam peak *cannot* be steered over *any* contiguous directional sector but only to a few isolated directions.

First, locate the critical points in $\{B_k^{(u_{\text{look}},v_{\text{look}},w_{\text{look}})}(u,v,w), \forall(u,v,w)\}$ for any algorithmically tuned $(u_{\text{look}}, v_{\text{look}}, w_{\text{look}})$ and any hardware-implemented k, subject to the constraint of

$$u^2(\theta,\phi) + v^2(\theta,\phi) + w^2(\theta) = 1, \quad \forall\theta, \forall\phi. \tag{12}$$

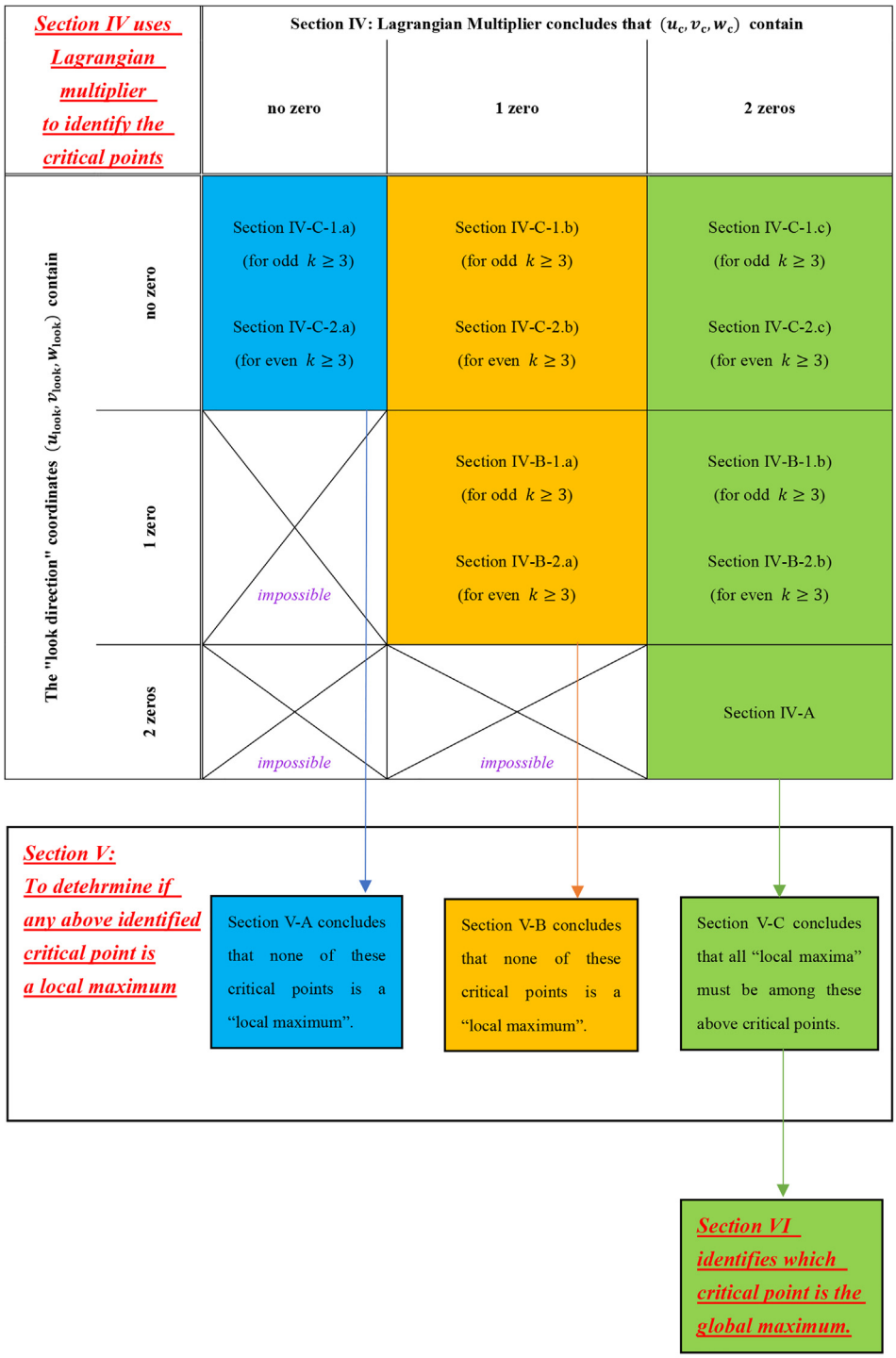

FIG. 3. (Color online) The logical flow of the analysis for the $k \geq 3$ directivity-order cases in Secs. IV–VI.

This can be achieved via the *method of Lagrange multiplier* by defining

$$L(u,v,w) \stackrel{\text{def}}{=} B_2^{(u_{\text{look}},v_{\text{look}},w_{\text{look}})}(u,v,w) + \lambda[u^2+v^2+w^2-1]. \tag{13}$$

Next, set

$$\begin{aligned} 0 &= \frac{\partial}{\partial u} L(u,v,w,\lambda)|_{(u,v,w)=(u_c,v_c,w_c)} \\ &= 2u_{\text{look}}^2 u_c + 2\lambda u_c, \end{aligned}$$

which can be satisfied only by

(i-u) $(u_c, \lambda) = (0, \lambda)$ for all $\lambda \in (-\infty, \infty)$, and/or
(ii-u) $(u_c, \lambda) = (u_c, -u_{\text{look}}^2)$ for all $u_c \in [-1, 1]$.

Similarly, $0 = (\partial/\partial v)L(u,v,w,\lambda)|_{(u,v,w)=(u_c,v_c,w_c)}$ implies that

(i-v) $(v_c, \lambda) = (0, \lambda)$ for all $\lambda \in (-\infty, \infty)$, and/or
(ii-v) $(v_c, \lambda) = (v_c, -v_{\text{look}}^2)$ for all $v_c \in [-1, 1]$.

Likewise, $0 = (\partial/\partial w)L(u,v,w,\lambda)|_{(u,v,w)=(u_c,v_c,w_c)}$ implies that

https://doi.org/10.1121/10.0009312

(i-w) $(w_c, \lambda) = (0, \lambda)$ for all $\lambda \in (-\infty, \infty)$, and/or
(ii-w) $(w_c, \lambda) = (w_c, -w_{look}^2)$ for all $w_c \in [-1, 1]$.

The beam-pattern's any local/global maximum must simultaneously satisfy all three sets: (i-u) and/or (ii-u), (i-v) and/or (ii-v), (i-w) and/or (ii-w). These six conditions vary with the look direction's Cartesian direction cosines, $\{u_{look}, v_{look}, w_{look}\}$. Depending on how many in $\{u_{look}, v_{look}, w_{look}\}$ have the same absolute magnitude—various disjoint sub-cases need be analyzed separately below.

A. If $|u_{look}| \neq |v_{look}| \neq |w_{look}|$

The above six conditions [i.e., (i-u)–(ii-u), (i-v)–(ii-v), (i-w)–(ii-w)] on $\{u_c, v_c, w_c, \lambda\}$ would require at least two zeros in $\{u_c, v_c, w_c\}$. This is proved by contradiction: consider two nonzeros in $\{u_c, v_c, w_c\}$, say, $u_c \neq 0$ and $v_c \neq 0$. Then, $\lambda = -u_{look}^2$ and $\lambda = -v_{look}^2$ must simultaneously hold, but these two λ expressions would contradict each other for $|u_{look}| \neq |v_{look}|$.

Furthermore, recall that the constraint (12) precludes u_c, v_c, w_c from being all zeros.

The two preceding paragraphs mean that $\{u_c, v_c, w_c\}$ must contain *exactly* two zeros, thereby implying only the six critical points of

$$(u_c, v_c, w_c) = (\pm 1, 0, 0), (0, \pm 1, 0), (0, 0, \pm 1).$$

[The ± 1 is due to the unity-constraint in Eq. (12).] These are the only candidates for the peak direction; no *contiguous* directional sector exists as a candidate peak direction.

To identify the peak direction from among these six candidates noted above, compare their heights:

$$|B_2^{(u_{look}, v_{look}, w_{look})}(\pm 1, 0, 0)| = u_{look}^2; \tag{14}$$

$$|B_2^{(u_{look}, v_{look}, w_{look})}(0, \pm 1, 0)| = v_{look}^2; \tag{15}$$

$$|B_2^{(u_{look}, v_{look}, w_{look})}(0, 0, \pm 1)| = w_{look}^2. \tag{16}$$

Hence,

$$(u_{peak}, w_{peak}, v_{peak}) = \begin{cases} (\pm 1, 0, 0) & \text{if } |u_{look}| > |v_{look}|, |w_{look}|; \\ (0, \pm 1, 0) & \text{if } |v_{look}| > |w_{look}|, |w_{look}|; \\ (0, 0, \pm 1) & \text{if } |w_{look}| > |u_{look}|, |v_{look}|. \end{cases} \tag{17}$$

Equation (17) is graphically represented in Fig. 4 in the polar-azimuthal bivariate coordinates.

In summary, when $u_{look} \neq v_{look} \neq w_{look}$, the $k = 2$ triad can*not* be beam steered incrementally over any *contiguous* directional sector, but the beam peak can only hop among 6 *discrete* directions, which generally differ from the nominal look direction.

B. If $|u_{look}| = |v_{look}| \neq |w_{look}|$

Here, the six conditions noted above [i.e., (i-u)–(ii-u), (i-v)–(ii-v), (i-w)–(ii-w)] require at least one zero in $\{u_c, v_c, w_c\}$. If furthermore there are two zeros in $\{u_c, v_c, w_c\}$, the corresponding critical points are $(\pm 1, 0, 0)$, $(0, \pm 1, 0), (0, 0, \pm 1)$. If there is exactly one zero in $\{u_c, v_c, w_c\}$, the corresponding critical points become a circle passing $(\pm 1, 0, 0)$ and $(0, \pm 1, 0)$. The preceding three sentences are proved in the following two sentences by contradiction: Suppose the simultaneous existence of three nonzeros in $\{u_c, v_c, w_c\}$. Then, $\lambda = -u_{look}^2 = -v_{look}^2$ and $\lambda = -w_{look}^2$ must simultaneously hold, but these two λ expressions contradict each other for $|u_{look}| = |v_{look}| \neq |w_{look}|$.

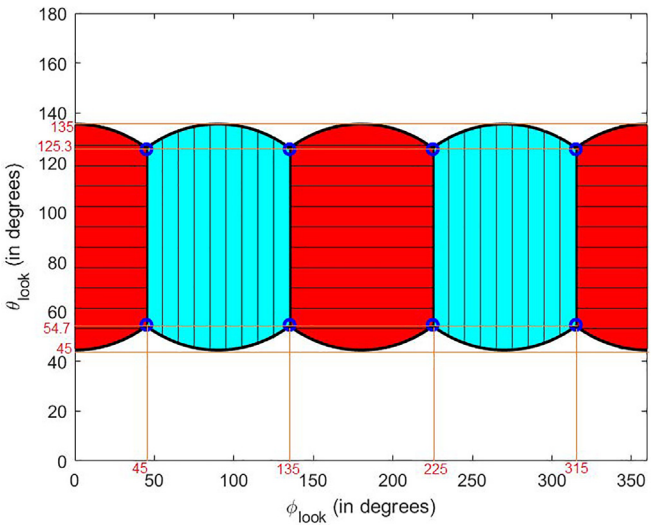

FIG. 4. (Color online) How the same peak direction results from an entire subsector of "look directions" for $k = 2$ and $k \geq 3$.

This contradiction implies either

(i) $u_c = v_c = 0$, or
(ii) $w_c = 0$.

The former implies that $(0, 0, \pm 1)$ are two critical points. The latter implies that $u_c^2 + v_c^2 = 1$ and $w_c = 0$, hence,

$$B_2^{(u_{look}, v_{look}, w_{look})}(u_c, v_c, w_c = 0) = u_{look}^2 = v_{look}^2.$$

If $|u_{look}| = |v_{look}| > |w_{look}|$, then the set of simultaneous maxima would constitute the circle of $u_{peak}^2 + v_{peak}^2 = 1$ on the horizontal x-y plane.

If $|u_{look}| = |v_{look}| < |w_{look}|$, then the local maxima must be $(0, 0, \pm 1)$.

C. If $|u_{look}| = |w_{look}| \neq |v_{look}|$

This case is analogous to that in Sec. III B with the y- and z-Cartesian direction cosines interchanged. This implies that the local maxima must be either the points $(0, \pm 1, 0)$ or the circle $u_{peak}^2 + w_{peak}^2 = 1$ on the vertical x-z plane (but not both).

D. If $|v_{look}| = |w_{look}| \neq |u_{look}|$

This case is similar to that in Sec. III B with the x- and z-Cartesian direction cosines interchanged. That is, the local maxima must be either the points $(\pm 1, 0, 0)$ or the circle $v_{peak}^2 + w_{peak}^2 = 1$ on the vertical y-z plane (but not both).

E. If $|u_{look}|=|v_{look}|=|w_{look}|$

Here, the beam-pattern amplitude $B_2^{(u_{look},v_{look},w_{look})}(u,v,w) = u_{look}^2 = v_{look}^2 = w_{look}^2$, which is a constant for all (u,v,w). This means that the triad's beam-pattern has a uniform height $\forall(\theta,\phi)$ without any peak or null.

F. Conclusion for directivity-order $k=2$

Sections III A–III E are summarized in Fig. 2 for a triad populated by the component-sensors with a directivity-order of $k=2$.

(i) The triad's SMF beam peak has three disjoint subcases: peaking at $(\pm1,0,0)$ for any look direction in the horizontally striped directional subsector (see Secs. III A and III D), peaking at $(0,\pm1,0)$ for the vertically striped subsector (see Secs. III A and III C), or peaking instead at $(0,0,\pm1)$ for any look direction in the blank subsector.

(ii) If the look direction lies on any thick dark curve, the peak direction constitutes a circle; please see Secs. III B–III D.

(iii) If the look direction is any of the eight hollow-circle points, the beam-pattern is a sphere with no peak; please see Sec. III E.

That is, the triad is *in*capable of steering its SMF beam peak over any contiguous directional subsector. The beam peak must be among the six detached directions of $(u_{peak},v_{peak},w_{peak}) \in \{(\pm1,0,0),(0,\pm1,0),(0,0,\pm1)\}$. As to which of these six directions—that depends on the nominal look direction $(u_{look},v_{look},w_{look})$.

IV. DIRECTIVITY-ORDER $k\geq3$: THE BEAM-PATTERN'S STATIONARY POINTS

Now, consider any hardware-implemented $k\geq3$, which is algorithmically tuned at $(u_{look},v_{look},w_{look})$. To locate where $B_k^{(u_{look},v_{look},w_{look})}(u,v,w)$ has extrema in the support region of $\{\forall(u,v,w)\}$: use the *method of Lagrange multiplier* while recalling the constraint of Eq. (12),

$$L(u,v,w)\overset{\text{def}}{=}B_k^{(u_{look},v_{look},w_{look})}(u,v,w)+\lambda[u^2+v^2+w^2-1], \tag{18}$$

whose partial derivatives are

$$\frac{\partial}{\partial u}L(u,v,w,\lambda)|_{(u,v,w)=(u_c,v_c,w_c)} = ku_{look}^k u_c^{k-1}+2\lambda u_c = 0, \tag{19}$$

$$\frac{\partial}{\partial v}L(u,v,w,\lambda)|_{(u,v,w)=(u_c,v_c,w_c)} = kv_{look}^k v_c^{k-1}+2\lambda v_c = 0, \tag{20}$$

$$\frac{\partial}{\partial w}L(u,v,w,\lambda)|_{(u,v,w)=(u_c,v_c,w_c)} = kw_{look}^k w_c^{k-1}+2\lambda w_c = 0. \tag{21}$$

The above would simplify to Eq. (13) for the $k=2$ case of Sec. III. However, with $k\geq3$ here, the next steps will involve many sub-cases and sub-sub-cases; please see Figs. 3 and 5. Therefore, the analysis here is more complicated than the $k=2$ directivity-order analysis in Sec. III.

Suppose that $u_{look}=0$ and $u_c\neq0$ in Eq. (19), then $\lambda=0$.

(1) If furthermore $v_{look}\neq0$ and $w_{look}\neq0$, Eqs. (20) and (21) would give $v_c=w_c=0$ and, thus, $B_k^{(u_{look}=0,v_{look}\neq0,w_{look}\neq0)}(u_c,v_c=0,w_c=0)=0$.

(2) If furthermore $v_{look}=0$ and $w_{look}\neq0$, Eq. (21) gives $w_c=0$, which implies that $B_k^{(u_{look}=0,v_{look}=0,w_{look}\neq0)}(u_c,v_c,w_c=0)=0$.

Together, (1) and (2) mean that when $u_{look}=0$, no critical point with $u_c\neq0$ can be a local/global maximum; thus, only $u_c=0$ needs further consideration below. Similar arguments hold for $v_{look}=0$ or $w_{look}=0$.

As u_c, v_c, and w_c could each be positive or negative, whether they are raised to an odd-k power or an even-k power—that would affect the subsequent analysis foundationally. Hence, the odd-k case and even-k case will be separately analyzed below.

For any *odd* $k\geq3$, Eqs. (19)–(21) would lead to

$$u_c\begin{cases}\in & \left\{0,\left(\frac{-2\lambda}{ku_{look}^k}\right)^{1/(k-2)}\right\} & \text{if } u_{look}\neq0;\\ = & 0 & \text{if } u_{look}=0;\end{cases} \tag{22}$$

$$v_c\begin{cases}\in & \left\{0,\left(\frac{-2\lambda}{kv_{look}^k}\right)^{1/(k-2)}\right\} & \text{if } v_{look}\neq0;\\ = & 0 & \text{if } v_{look}=0;\end{cases} \tag{23}$$

$$w_c\begin{cases}\in & \left\{0,\left(\frac{-2\lambda}{kw_{look}^k}\right)^{1/(k-2)}\right\} & \text{if } w_{look}\neq0;\\ = & 0 & \text{if } w_{look}=0.\end{cases} \tag{24}$$

Any critical point must simultaneously satisfy Eqs. (12) and (22)–(24), if k is odd and exceeds two. Furthermore, whether any entry in $\{u_{look},v_{look},w_{look}\}$ equals zero—that would radically change the critical points' set of values.

For any *even* $k\geq4$, Eqs. (19)–(21) would lead instead to

$$u_c\begin{cases}\in & \left\{0,\pm\left(\frac{-2\lambda}{ku_{look}^k}\right)^{1/(k-2)}\right\} & \text{if } u_{look}\neq0;\\ = & 0 & \text{if } u_{look}=0;\end{cases} \tag{25}$$

$$v_c\begin{cases}\in & \left\{0,\pm\left(\frac{-2\lambda}{kv_{look}^k}\right)^{1/(k-2)}\right\} & \text{if } v_{look}\neq0;\\ = & 0 & \text{if } v_{look}=0;\end{cases} \tag{26}$$

$$w_c\begin{cases}\in & \left\{0,\pm\left(\frac{-2\lambda}{kw_{look}^k}\right)^{1/(k-2)}\right\} & \text{if } w_{look}\neq0;\\ = & 0 & \text{if } w_{look}=0.\end{cases} \tag{27}$$

https://doi.org/10.1121/10.0009312

Section #	Under These Conditions			Then	Local Maxima Subsequently Derived in Section #
	$k \geq 3$, and k is	# of zeros in $\{u_{\text{look}}, v_{\text{look}}, w_{\text{look}}\}$	# of zeros in $\{u_c, v_c, w_c\}$	critical points $(u_c, v_c, w_c) =$	
IV A	even or odd	2	2	$(0,0,\pm1)$, if $u_{\text{look}} = v_{\text{look}} = 0$; $(0,\pm1,0)$, if $u_{\text{look}} = w_{\text{look}} = 0$; $(\pm1,0,0)$, if $v_{\text{look}} = w_{\text{look}} = 0$.	
IV B 1 a	odd	1	1	$\pm\frac{(0,\hat{v},\hat{w})}{\sqrt{\hat{v}^2+\hat{w}^2}}$, if $u_{\text{look}} = 0$; $\pm\frac{(\hat{u},0,\hat{w})}{\sqrt{\hat{u}^2+\hat{w}^2}}$, if $v_{\text{look}} = 0$; $\pm\frac{(\hat{u},\hat{v},0)}{\sqrt{\hat{u}^2+\hat{v}^2}}$, if $w_{\text{look}} = 0$.	V B
IV B 1 b	odd	1	2	$(0,\pm1,0),(0,0,\pm1)$, if $u_{\text{look}} = 0$; $(\pm1,0,0),(0,0,\pm1)$, if $v_{\text{look}} = 0$; $(\pm1,0,0),(0,\pm1,0)$, if $w_{\text{look}} = 0$.	
IV B 2 a	even	1	1	$\frac{(0,\ \pm\hat{v},\ \pm\hat{w})}{\sqrt{\hat{v}^2+\hat{w}^2}}$, if $u_{\text{look}} = 0$; $\frac{(\pm\hat{u},\ 0,\ \pm\hat{w})}{\sqrt{\hat{u}^2+\hat{w}^2}}$, if $v_{\text{look}} = 0$; $\frac{(\pm\hat{u},\ \pm\hat{v},\ 0)}{\sqrt{\hat{u}^2+\hat{v}^2}}$, if $w_{\text{look}} = 0$.	V B
IV B 2 b	even	1	2	$(0,\pm1,0),(0,0,\pm1)$, if $u_{\text{look}} = 0$; $(\pm1,0,0),(0,0,\pm1)$, if $v_{\text{look}} = 0$; $(\pm1,0,0),(0,\pm1,0)$, if $w_{\text{look}} = 0$.	
IV C 1 a	odd	0	0	$\frac{\pm(\hat{u},\hat{v},\hat{w})}{\sqrt{\hat{u}^2+\hat{v}^2+\hat{w}^2}}$	V A
IV C 1 b	odd	0	1	$\pm\frac{(0,\hat{v},\ \hat{w})}{\sqrt{\hat{v}^2+\hat{w}^2}}$, and $\pm\frac{(\hat{u},0,\ \hat{w})}{\sqrt{\hat{u}^2+\hat{w}^2}}$, and $\pm\frac{(\hat{u},\hat{v},0)}{\sqrt{\hat{u}^2+\hat{v}^2}}$.	V B
IV C 1 c	odd	0	2	$(\pm1,0,0),(0,\pm1,0)$, and $(0,0,\pm1)$	
IV C 2 a	even	0	0	$\frac{(\pm\hat{u},\pm\hat{v},\pm\hat{w})}{\sqrt{\hat{u}^2+\hat{v}^2+\hat{w}^2}}$	V A
IV C 2 b	even	0	1	$\frac{(0,\pm\hat{v},\pm\hat{w})}{\sqrt{\hat{v}^2+\hat{w}^2}}$, and $\frac{(\pm\hat{u},0,\pm\hat{w})}{\sqrt{\hat{u}^2+\hat{w}^2}}$, and $\frac{(\pm\hat{u},\pm\hat{v},0)}{\sqrt{\hat{u}^2+\hat{v}^2}}$.	V B
IV C 2 c	even	0	2	$(\pm1,0,0),(0,\pm1,0)$, and $(0,0,\pm1)$	

FIG. 5. (Color online) The critical points for all possible sub-cases in Sec. IV, where $k \geq 3$.

Note the ±1 in Eqs. (25)–(27) but there is no ±1 in Eqs. (22)–(24). Any critical point must simultaneously satisfy Eqs. (12) and (25)–(27), if k is even and exceeds two. Moreover, whether any entry in $\{u_{\text{look}}, v_{\text{look}}, w_{\text{look}}\}$ equals zero—that would essentially alter the critical points' set of values.

In light of all of the above, the (u_c, v_c, w_c) scenario here (for $k \geq 3$) is more complicated than in Sec. III for $k = 2$. Here, for $k \geq 3$, the subsequent analysis will be considered through many sub-cases, which are differentiated by

(a) whether k is odd or even,
(b) the number of zero entries in $\{u_{\text{look}}, v_{\text{look}}, w_{\text{look}}\}$, and
(c) the number of zero entries in $\{u_c, v_c, w_c\}$.

The above leads to very different mathematical forms, each of which needs separate handling.

These sub-cases have been summarized in Figs. 3 and 5. Each sub-case's conclusion is summarized on a separate row in Fig. 5. The far-left column in Fig. 5 indicates the section in which the detailed derivation may be found; and $\hat{u}$, $\hat{v}$,

and $\hat{w}$ are defined as $u_{\text{look}}^{-k/(k-2)}$, $v_{\text{look}}^{-k/(k-2)}$, and $w_{\text{look}}^{-k/(k-2)}$, respectively. Only those sub-cases in the striped cells can lead to actual peak directions.

A. If exactly two in $\{u_{\text{look}}, v_{\text{look}}, w_{\text{look}}\}$ are zero

Consider first the special case of $u_{\text{look}} = v_{\text{look}} = 0$; the other special cases of $u_{\text{look}} = w_{\text{look}} = 0$ or $v_{\text{look}} = w_{\text{look}} = 0$ are analogous and will be analyzed later.

If $u_{\text{look}} = v_{\text{look}} = 0$, then implicitly $w_{\text{look}} = \pm 1$ due to the constraint in Eq. (12). With the beamformer set toward the look directions of $(0, 0, \pm 1)$, the beam-pattern's magnitude equals

$$|B_k^{(0,0,\pm 1)}(u, v, w)| = |w^k|, \tag{28}$$

which attains its maximum of

$$\max_{(u,v,w)} |B_k^{(0,0,\pm 1)}(u, v, w)| = \max_{\forall w \in [-1,1]} |w^k| = 1 \tag{29}$$

at $w = w_{\text{peak}} = \pm 1$. That is, the beam must peak at $(u_{\text{peak}}, v_{\text{peak}}, w_{\text{peak}}) = (0, 0, \pm 1)$, thus, exactly matching the preset look direction of $(u_{\text{look}}, v_{\text{look}}, w_{\text{look}}) = (0, 0, \pm 1)$. This holds $\forall k \geq 1$.

Similarly, the special case of $v_{\text{look}} = w_{\text{look}} = 0$ gives a peak direction of $(u_{\text{peak}}, v_{\text{peak}}, w_{\text{peak}}) = (\pm 1, 0, 0)$, which precisely matches the preset look direction of $(u_{\text{look}}, v_{\text{look}}, w_{\text{look}}) = (\pm 1, 0, 0)$.

Likewise, the special case of $u_{\text{look}} = w_{\text{look}} = 0$ yields a peak direction of $(u_{\text{peak}}, v_{\text{peak}}, w_{\text{peak}}) = (0, \pm 1, 0)$, exactly matching the preset look direction of $(u_{\text{look}}, v_{\text{look}}, w_{\text{look}}) = (0, \pm 1, 0)$.

In summary, $(u_{\text{peak}}, v_{\text{peak}}, w_{\text{peak}}) = \pm(u_{\text{look}}, v_{\text{look}}, w_{\text{look}})$ if $(u_{\text{look}}, v_{\text{look}}, w_{\text{look}}) \in \{(\pm 1, 0, 0), (0, \pm 1, 0), (0, 0, \pm 1)\}$.

B. If exactly one zero in $\{u_{\text{look}}, v_{\text{look}}, w_{\text{look}}\}$

From Eqs. (22)–(24) for any odd $k \geq 3$, and from Eqs. (25)–(27) for any even $k \geq 4$: $u_{\text{look}} = 0$ implies $u_c = 0$, and similarly with v_{look} and w_{look}.

Due to the interaxial permutational analogies among the x, y, and z axes, the following analysis will focus on the case of $(u_{\text{look}}, v_{\text{look}}, w_{\text{look}}) = (0, \neq 0, \neq 0)$, for example. The other cases of $(u_{\text{look}}, v_{\text{look}}, w_{\text{look}}) = (\neq 0, 0, \neq 0)$ or $(u_{\text{look}}, v_{\text{look}}, w_{\text{look}}) = (\neq 0, \neq 0, 0)$ would be likewise.

The odd-k sub-case will be analyzed in Sec. IV B 1 with the even-k sub-case analyzed in Sec. IV B 2.

1. Odd $k \geq 1$

Although $u_{\text{look}} = 0$ in Eq. (22) restricts u_c to zero, Eq. (23) allows v_c to be either zero or nonzero, and Eq. (24), likewise, permits w_c to be either zero or nonzero. The sub-case of both v_c and w_c being nonzero will be considered in Sec. IV B 1 a, whereas the other sub-case of exactly one of v_c and w_c being zero will be considered in Sec. IV B 1 b. [Constraint (12) precludes both v_c and w_c from being zero, in addition to precluding u_c from being zero.]

a. Both v_c and w_c are nonzero. With $k \geq 1$ and odd,

$$|B_k^{(u_{\text{look}}, v_{\text{look}}, w_{\text{look}})}(u, v, w)| = |B_k^{(u_{\text{look}}, v_{\text{look}}, w_{\text{look}})}(-u, -v, -w)|. \tag{30}$$

This implies that either both $\pm(u_c, v_c, w_c)$ are local maxima of $|B_k^{(u_{\text{look}}, v_{\text{look}}, w_{\text{look}})}(u, v, w)|$ or neither is.

The substitution of $u_{\text{look}} = 0$ into Eqs. (22)–(24) gives

$$u_c = 0, \tag{31}$$

$$v_c = \left(\frac{-2\lambda}{k {v_{\text{look}}}^k}\right)^{1/(k-2)}, \tag{32}$$

$$w_c = \left(\frac{-2\lambda}{k {w_{\text{look}}}^k}\right)^{1/(k-2)}. \tag{33}$$

Substitution of the above three equalities into Eq. (12) yields

$$\left(\frac{-2\lambda}{k}\right)^{1/(k-2)} = \frac{\pm 1}{\sqrt{v_{\text{look}}^{-2k/(k-2)} + w_{\text{look}}^{-2k/(k-2)}}}. \tag{34}$$

Last, substitute Eq. (34) into Eqs. (31)–(33) to produce

$$(u_c, v_c, w_c) = \pm \frac{\left(0, v_{\text{look}}^{-k/(k-2)}, w_{\text{look}}^{-k/(k-2)}\right)}{\sqrt{{v_{\text{look}}}^{-2k/(k-2)} + {w_{\text{look}}}^{-2k/(k-2)}}}. \tag{35}$$

b. Exactly one of v_c and w_c is zero. Suppose v_c is zero in addition to $u_c = 0$, but w_c remains nonzero. Then $(u_c, v_c, w_c) = (0, 0, \pm 1)$ due to the constraint in Eq. (12).

If, instead, $w_c = 0$ in addition to $u_c = 0$, but v_c is nonzero, then $(u_c, v_c, w_c) = (0, \pm 1, 0)$ is also due to the constraint in Eq. (12).

2. Even $k \geq 4$

a. Both v_c and w_c are nonzero. The substitution of $u_{\text{look}} = 0$ into Eqs. (25)–(27) gives

$$u_c = 0, \tag{36}$$

$$v_c = \pm\left(\frac{-2\lambda}{k {v_{\text{look}}}^k}\right)^{1/(k-2)}, \tag{37}$$

$$w_c = \pm\left(\frac{-2\lambda}{k {w_{\text{look}}}^k}\right)^{1/(k-2)}. \tag{38}$$

The λ expression Eq. (34) holds whether $k \geq 3$ is odd or even. Substitute that Eq. (34) into Eqs. (36)–(38) to give

$$(u_c, v_c, w_c) = \frac{\left(0, \pm v_{\text{look}}^{-k/(k-2)}, \pm w_{\text{look}}^{-k/(k-2)}\right)}{\sqrt{{v_{\text{look}}}^{-2k/(k-2)} + {w_{\text{look}}}^{-2k/(k-2)}}}. \tag{39}$$

As expected, Eq. (39) is the same as Eq. (35).

https://doi.org/10.1121/10.0009312

Either all four directions in $(0, \pm v_c, \pm w_c)$ are local maxima or none is. This is because $\pm$ makes no difference in $|B_k^{(u_{look}, v_{look}, w_{look})}(\pm u, \pm v, \pm w)|$.

b. Exactly one of v_c and w_c is zero. Suppose v_c is zero in addition to $u_c = 0$ but w_c remains nonzero. Then, $(u_c, v_c, w_c) = (0, 0, \pm 1)$ due to the constraint in Eq. (2). If w_c, instead, is zero in addition to $u_c = 0$ but v_c remains nonzero, then $(u_c, v_c, w_c) = (0, \pm 1, 1)$, which is due also to the constraint in Eq. (12).

Either all four directions in $(0, \pm v_c, \pm w_c)$ are all local maxima or none is. This is because $\pm$ makes no difference in $|B_k^{(u_{look}, v_{look}, w_{look})}(\pm u, \pm v, \pm w)|$.

C. If no zero in $\{u_{look}, v_{look}, w_{look}\}$

From Eqs. (22)–(24) for any odd $k \geq 3$ and from Eqs. (25)–(27) for any even $k \geq 4$, a nonzero u_{look} would not preclude u_c from being zero or nonzero.

The odd-k sub-case will be analyzed in Sec. IV C 1, whereas the even-k sub-case will be analyzed in Sec. IV C 2.

To facilitate the subsequent analysis: Substitute the (u_c, v_c, w_c) of either the odd-k's Eqs. (22)–(24) or the even-k's Eqs. (25)–(27) for $(u(\theta, \phi), v(\theta, \phi), w(\theta, \phi))$ in the constraint of Eq. (12). Either case would give

$$\left(\frac{-2\lambda}{k}\right)^{1/(k-2)} = \begin{cases} \dfrac{\pm 1}{\sqrt{{u_{look}}^{-2k/(k-2)} + {v_{look}}^{-2k/(k-2)} + {w_{look}}^{-2k/(k-2)}}} & \text{if } u_c, v_c, w_c \neq 0; \\ \dfrac{\pm 1}{\sqrt{{v_{look}}^{-2k/(k-2)} + {w_{look}}^{-2k/(k-2)}}} & \text{if } u_c = 0,\ v_c, w_c \neq 0. \end{cases} \tag{40}$$

The numerator's signs give two candidate directions [for the actual peak(s)] at diametrically opposite directions.

1. Odd k

Three sub-cases exist as to how many zeros in $\{u_c, v_c, w_c\}$—no zero, one zero, or two zeros. These three sub-cases are discussed one by one below. [Recall that the all-zeros case is disallowed by the constraint in Eq. (12).]

a. If u_c, v_c, and w_c are all nonzero in Eqs. (22)–(24). Substitute Eq. (40) into Eqs. (22)–(24) to yield

$$(u_c, v_c, w_c) = \frac{\pm\left({u_{look}}^{-k/(k-2)}, {v_{look}}^{-k/(k-2)}, {w_{look}}^{-k/(k-2)}\right)}{\sqrt{{u_{look}}^{-2k/(k-2)} + {v_{look}}^{-2k/(k-2)} + {w_{look}}^{-2k/(k-2)}}}. \tag{41}$$

The directions specified in Eq. (41) are only a subset of all of the peak-candidates.

Recall the beam-pattern magnitude's diametric symmetry described in Eq. (6). Either both $\pm(u_c, v_c, w_c)$ are a local maximum of the magnitude beam-pattern or neither is.

b. Exactly one of $\{u_c, v_c, w_c\}$ is zero. Due to the mathematical similarity of u, v, and w, take $u_c = 0$ such that

$$(u_c, v_c, w_c) = \pm \frac{\left(0, {v_{look}}^{-k/(k-2)}, {w_{look}}^{-k/(k-2)}\right)}{\sqrt{{v_{look}}^{-2k/(k-2)} + {w_{look}}^{-2k/(k-2)}}}. \tag{42}$$

As expected, Eq. (42) is the same as Eqs. (35) and (39).

Recall the beam-pattern magnitude's diametric symmetry described in Eq. (6). Either both $\pm(u_c, v_c, w_c)$ are local maximum of the magnitude beam-pattern or neither is.

Four other peak-candidates exist, corresponding to $v_c = 0$ or $w_c = 0$.

c. Exactly two of $\{u_c, v_c, w_c\}$ are zero. Three sub-cases exist such that

(1) if $v_c = w_c = 0$ but $u_c \neq 0$: $(u_c, v_c, w_c) = (\pm 1, 0, 0)$;
(2) if $u_c = w_c = 0$ but $v_c \neq 0$: $(u_c, v_c, w_c) = (0, \pm 1, 0)$; or
(3) if $v_c = u_c = 0$ but $w_c \neq 0$: $(u_c, v_c, w_c) = (0, 0, \pm 1)$.

2. Even k

Recalling Eqs. (25)–(27), three sub-cases exist and will be separately analyzed below.

a. If u_c, v_c, and w_c are all nonzero in Eqs. (22)–(24). Substitute Eq. (40) into Eqs. (25)–(27) to yield

$$(u_c, v_c, w_c) = \frac{\left(\pm {u_{look}}^{-k/(k-2)}, \pm {v_{look}}^{-k/(k-2)}, \pm {w_{look}}^{-k/(k-2)}\right)}{\sqrt{{u_{look}}^{-2k/(k-2)} + {v_{look}}^{-2k/(k-2)} + {w_{look}}^{-2k/(k-2)}}}. \tag{43}$$

Here, Eq. (43) points toward the peak-candidates.

Recall the eightfold symmetry in Eq. (7) for any even $k \geq 4$. Hence, either all eight of $(\pm u_c, \pm v_c, \pm w_c)$ are local maxima of the magnitude beam-pattern or none is.

b. Exactly one of $\{u_c, v_c, w_c\}$ is zero. Due to the mathematical similarity of u, v, and w, take $u_c = 0$:

$$u_c = 0, \tag{44}$$

$$v_c = \pm \frac{{v_{look}}^{-k/(k-2)}}{\sqrt{{v_{look}}^{-2k/(k-2)} + {w_{look}}^{-2k/(k-2)}}}, \tag{45}$$

$$w_c = \pm \frac{{w_{look}}^{-k/(k-2)}}{\sqrt{{v_{look}}^{-2k/(k-2)} + {w_{look}}^{-2k/(k-2)}}}. \tag{46}$$

For $u_c = 0$, there are $(0, \pm v_c, \pm w_c)$. And there are eight other points for $v_c = 0$ and $w_c = 0$.

For even $k \geq 4$, the following symmetry holds:

$$|B_k^{(u_{look}, v_{look}, w_{look})}(u, v, w)| = |B_k^{(u_{look}, v_{look}, w_{look})}(\pm u, \pm v, \pm w)|. \tag{47}$$

Thus, if (u_c, v_c, w_c) is not a local maximum of $|B_k^{(u_{look}, v_{look}, w_{look})}(u, v, w)|, \forall k \geq 4$, then neither are the following seven points: $(-u_c, v_c, w_c), (-u_c, -v_c, w_c), (-u_c, v_c, -w_c), (-u_c, -v_c, -w_c), (u_c, -v_c, w_c), (u_c, -v_c, -w_c), (u_c, v_c, -w_c)$.

c. Exactly two of $\{u_c, v_c, w_c\}$ *are zero.* If $v_c = w_c = 0$ but u_c is nonzero, then $(u_c, v_c, w_c) = (\pm 1, 0, 0)$; if $u_c = w_c = 0$ but v_c is nonzero, then $(u_c, v_c, w_c) = (0, \pm 1, 0)$; if $v_c = u_c = 0$ but w_c is nonzero, then $(u_c, v_c, w_c) = (0, 0, \pm 1)$.

V. DIRECTIVITY-ORDER $k \geq 3$: THE BEAM-PATTERN'S LOCAL MAXIMA

The beam-pattern's peak direction (i.e., global maximum) must necessarily be a local maximum, which, in turn, must be a critical point. All critical points have already been identified in Sec. IV for any directivity-order of $k \geq 3$. This section will determine which of these critical points are local maxima and which are not. Please refer back to Fig. 3 for a macroscopic overview of the logical flow among Secs. IV–VI.

The many sub-cases in Sec. IV fall into only three groups for the present purpose of testing which critical point is a local maximum:

(1) $\{u_c, v_c, w_c\}$ contains no zero: These sub-cases are the earlier Eq. (41) in Sec. IV C 1 a and Eq. (43) in Sec. IV C 2 a. Section V A will deal with this group of cases.
(2) $\{u_c, v_c, w_c\}$ contains exactly one zero: These sub-cases are the earlier Eq. (35) in Sec. IV B 1 a, Eq. (39) in Sec. IV B 2 a, Eq. (42) in Sec. IV C 1 b, and Eqs. (44)–(46) in Sec. IV C 2 b. Section V B will deal with this group of cases.
(3) $\{u_c, v_c, w_c\}$ contains exactly one zero: These sub-cases are the earlier Secs. IV A, IV B 1 b, IV B 2 b, IV C 1 c and IV C 2 c. Section V C will deal with this group of cases.

The "second partial derivative test" will be used below but in a not-so-straightforward manner. This indirectness is because the second partial derivative test is for unconstrained optimization, whereas the beam-pattern's three Cartesian direction cosines of u, v, and w are constrained through Eq. (12).

A. If no zero in $\{u_c, v_c, w_c\}$

Section V A will mathematically prove that all of the critical points with no zero in $\{u_c, v_c, w_c\}$ must be a local *minimum* and, hence, not a global maximum. The proof is given in the rest of Sec. V A.

The beam-pattern's three Cartesian direction cosines of u, v, and w are functionally dependent, inter-related through the constraint in Eq. (12). Thus, the second partial derivative test cannot be applied straightforwardly here by regarding u, v, and w as three degrees-of-freedom. Nonetheless, any local *minimum* of the unconstrained $|B_k^{(u_{look}, v_{look}, w_{look})}(u, v, w)|$ cannot possibly be a local *maximum* of the constrained $|B_k^{(u_{look}, v_{look}, w_{look})}(u, v, w)|$. The following will first prove that all of the critical points here are local *minima* when without constraint and, therefore, cannot be a local *maximum* when with constraint.

According to the second partial derivative test: If a multivariate function's Hessian matrix is invertible and positive definite at a critical point, that critical point must be a local *minimum*. For the trivariate function of $B_k^{(u_{look}, v_{look}, w_{look})}(u, v, w)$: among its nine second-order partial derivatives, six are zero and only three are nonzero. Those three are $\partial^2/\partial u \partial u$, $\partial^2/\partial v \partial v$, and $\partial^2/\partial w \partial w$. Hence, the beam-pattern's Hessian matrix is diagonal, and the 3×3 Hessian matrix's eigenvalues are its diagonal entries,

$$\frac{\partial^2}{\partial \xi \partial \xi} B_k^{(u_{look}, v_{look}, w_{look})}(u, v, w) = k(k-1) \xi_{look}^k \xi^{k-2}, \tag{48}$$

for all $\xi \in \{u, v, w\}$. At the critical point of

$$(u_c, v_c, w_c) = \frac{\left(u_{look}^{-k/(k-2)}, v_{look}^{-k/(k-2)}, w_{look}^{-k/(k-2)}\right)}{\left(u_{look}^{-2k/(k-2)} + v_{look}^{-2k/(k-2)} + w_{look}^{-2k/(k-2)}\right)^{1/2}}, \tag{49}$$

the aforementioned eigenvalues in Eq. (48) become

$$\frac{\partial^2}{\partial \xi \partial \xi} B_k^{(u_{look}, v_{look}, w_{look})}(u_c, v_c, w_c) = \frac{k(k-1)}{\left(u_{look}^{-2k/(k-2)} + v_{look}^{-2k/(k-2)} + w_{look}^{-2k/(k-2)}\right)^{(k-2)/2}} > 0. \tag{50}$$

Hence, the Hessian matrix is positive definite; all of the critical points of the form in Eq. (49) [on account of the symmetry properties in Eqs. (6) and (7)] must each be a local *minimum* in the unconstrained case.

The aforementioned analyzes the *amplitude* pattern $B_k^{(u_{look}, v_{look}, w_{look})}(u, v, w)$. The following will show that the critical points in either Eq. (41) or Eq. (43) are local minima of the magnitude pattern $|B_k^{(u_{look}, v_{look}, w_{look})}(u_c, v_c, w_c)|$. At these critical points,

$$B_k^{(u_{look}, v_{look}, w_{look})}(u_c, v_c, w_c) = \frac{u_{look}^{-2k/(k-2)} + v_{look}^{-2k/(k-2)} + w_{look}^{-2k/(k-2)}}{\left(u_{look}^{-2k/(k-2)} + v_{look}^{-2k/(k-2)} + w_{look}^{-2k/(k-2)}\right)^{k/2}} > 0 \tag{51}$$

because the numerator's every term has been raised to an even power.

The above has analytically proved that all of the critical points of the form Eq. (49) are a local *minimum* in the unconstrained case and, therefore, *not* a local *maximum* under constraint (12).

https://doi.org/10.1121/10.0009312

B. If exactly one zero in $\{u_c, v_c, w_c\}$

Section V B (in its entirety) will mathematically prove that all of the critical points with exactly one zero in $\{u_c, v_c, w_c\}$ must be a local *minimum* and, hence, not a global maximum. The rest of Sec. V B will prove this.

As in Sec. V A, the second partial derivative test cannot be applied straightforwardly here by regarding u, v, and w as three degrees-of-freedom because only two degrees-of-freedom exist among these three. So, the second partial derivative test will also be applied indirectly here but in a way that is different from that in Sec. V A. The present approach is as follows:

(i) Consider two constraints:
(A) $u^2 + v^2 + w^2 = 1$; and
(B) $u = 0$ and $v^2 + w^2 = 1$. This constraint is met by all of the critical points considered in Sec. V B.
Constraint (B) is obviously a restricted case of constraint (A). Suppose the beam-pattern magnitude, $|B_k^{(u_{look}, v_{look}, w_{look})}(u_c, v_c, w_c)|$, has a critical point (u_c, v_c, w_c) that satisfies (B). That (u_c, v_c, w_c) must also satisfy (A).

(ii) Prove (u_c, v_c, w_c) to be a local *minimum* of the beam-pattern magnitude under constraint (B). Then, that (u_c, v_c, w_c) must not be a local *maximum* within the larger set defined by constraint (A).

Under constraint (B),

$$B_k^{(u_{look}, v_{look}, w_{look})}(u_c = 0, v_c, w_c) = v_{look}^k v_c^k + w_{look}^k w_c^k. \quad (52)$$

Its 2×2 Hessian matrix (when without constraint) would be diagonal because the off diagonal entries for $\partial^2/\partial v \partial w$ and $\partial^2/\partial w \partial v$ both equal zero. The Hessian matrix's two eigenvalues are, thus, its diagonal entries as in Eq. (48) but for only $\xi = v, w$.

At the critical point of

$$(u_c, v_c, w_c) = \frac{\left(0,\ v_{look}^{-k/(k-2)},\ w_{look}^{-k/(k-2)}\right)}{\left(v_{look}^{-2k/(k-2)} + w_{look}^{-2k/(k-2)}\right)^{1/2}}, \quad (53)$$

the aforementioned eigenvalues in Eq. (48) become

$$\frac{\partial^2}{\partial \xi \partial \xi} B_k^{(u_{look}, v_{look}, w_{look})}(u_c = 0, v_c, w_c) = \frac{k(k-1)}{\left(v_{look}^{-2k/(k-2)} + w_{look}^{-2k/(k-2)}\right)^{(k-2)/2}} > 0. \quad (54)$$

Hence, the Hessian matrix is positive definite, and all of the critical points of the form Eq. (53) [on account of the symmetry properties in Eqs. (6) and (7)] must each be a local *minimum* of the beam-pattern amplitude when under constraint: $u = 0$ (v, w unconstrained), hence, a local *minimum* of the beam-pattern amplitude when under constraint (B) where $u = 0$ and v and w are constrained.

The preceding analyzes the *amplitude* pattern $B_k^{(u_{look}, v_{look}, w_{look})}(u, v, w)$. The following will show that the critical points are not any local maximum of the magnitude pattern $|B_k^{(u_{look}, v_{look}, w_{look})}(u_c, v_c, w_c)|$. At these critical points,

$$B_k^{(u_{look}, v_{look}, w_{look})}(u_c = 0, v_c, w_c) = \frac{v_{look}^{-2k/(k-2)} + w_{look}^{-2k/(k-2)}}{\left(v_{look}^{-2k/(k-2)} + w_{look}^{-2k/(k-2)}\right)^{k/2}} > 0 \quad (55)$$

because the numerator's every term has been raised to an even power.

The above has analytically proved that all of the critical points of the form of Eq. (53) must be a local *minimum* when under a more restricted constraint (B) and, therefore, can*not* be a local *maximum* when under constraint (A).

C. If exactly two zeros in $\{u_c, v_c, w_c\}$

Sections V A and V B have each shown that all of their sub-cases are *not* producing any local maximum. Therefore, any local/global maxima must be in the only remaining group (3), mentioned at the start of the Sec. V.

VI. DIRECTIVITY-ORDER $k \geq 3$: THE BEAM-PATTERN'S ACTUAL PEAK DIRECTIONS

This section will prove that for any $k \geq 3$, the triad cannot be steered incrementally over any contiguous directional sector but can only hop among six discrete directions.

Recall that for directivity-orders $k \geq 3$, Sec. IV has analytically derived the set of critical points for each possible setting of k, $\{u_{look}, v_{look}, w_{look}\}$, and $\{u_c, v_c, w_c\}$. Among these critical points, Sec. V has proved that the local maxima could only be among $\{(\pm 1, 0, 0), (0, \pm 1, 0), (0, 0, \pm 1)\}$. Please refer back to Fig. 3.

Which of these are global maxima? This can be determined by comparing their beam heights,

$$|B_k^{(u_{look}, v_{look}, w_{look})}(\pm 1, 0, 0)| = |u_{look}|^k; \quad (56)$$

$$|B_k^{(u_{look}, v_{look}, w_{look})}(0, \pm 1, 0)| = |v_{look}|^k; \quad (57)$$

$$|B_k^{(u_{look}, v_{look}, w_{look})}(0, 0, \pm 1)| = |w_{look}|^k. \quad (58)$$

Hence,

$$(u_{peak}, w_{peak}, v_{peak}) = \begin{cases} (\pm 1, 0, 0) & \text{if } |u_{look}| > |v_{look}|, |w_{look}|; \\ (0, \pm 1, 0) & \text{if } |v_{look}| > |u_{look}|, |w_{look}|; \\ (0, 0, \pm 1) & \text{if } |w_{look}| > |u_{look}|, |v_{look}|. \end{cases} \quad (59)$$

The conclusion above for $k \geq 3$ is identical to that in Eq. (17) for $k = 2$. This is summarized in Fig. 4.

(i) For any $k \geq 2$: The triad's SMF beam peak has three disjoint cases: peaking at $(\pm 1, 0, 0)$ for any look direction in the horizontally striped directional sector (see Secs. III A, III D, and VI), or peaking at $(0, \pm 1, 0)$ for the vertically striped sector (see Secs.

III A, III C, and VI), or peaking instead at $(0, 0, \pm 1)$ for any look direction in the blank sector.

(ii) For $k \geq 3$: If the look direction is on any thick dark curve, four peaks exist simultaneously; please see Eqs. (56)–(58). If the look direction is any of the eight hollow-circle points, six peaks exist simultaneously; please see Eqs.(56)–(58).

VII. CONCLUSION

Given the practical beamforming successes realized by the triad comprising orthogonally collocated *first*-order figure-8 microphones/hydrophones, a simple-minded expectation is that the *second*-order and *higher*-order figure-8 sensors (being sharper in their individual gain pattern) would make the triad's SMF beam acute while retaining the first-order case's steerability. Instead, this paper analytically exposes one critical shortcoming of these higher-order cases: their triad's SMF beam peak has limited maneuverability. Whereas the first directivity-order of $k = 1$ facilitates the triad to steer toward any polar-azimuthal direction (and to do so without any pointing bias), any higher directivity-order of $k \geq 2$ would permit the beam peak only to hop among the six discrete directions of $(u_{\text{peak}}, w_{\text{peak}}, v_{\text{peak}}) \in \{(\pm 1, 0, 0), (0, \pm 1, 0), (0, 0, \pm 1)\}$. In this sense, the $k = 1$ case is preferable over all of the $k \geq 2$ cases.

This finding echoes a complementary discovery in Ref. 28 for a *pair* of identical, collocated but orthogonally oriented figure-8 sensors of any equal directivity-order that (i) only the $k = 1$ directivity-order facilitates full steerability of the SMF beam to any look direction, and (ii) at any $k \geq 2$, the beam peak can only hop to $(u_{\text{peak}}, w_{\text{peak}}, v_{\text{peak}}) \in \{(\pm 1, 0, 0), (0, \pm 1, 0)\}$. Therefore, relative to the pair in Ref. 28 at $k \geq 2$, the present triad at $k \geq 2$, here, only adds two potential peaks at $(0, 0, \pm 1)$.

ACKNOWLEDGMENTS

S.S.D. and K.T.W. were supported, in part, by the National Natural Science Foundation of China via Grant No. 62071018. Y.S. was supported, in part, by the National Natural Science Foundation of China via Grant No. 61801128. The authors would like to thank Dr. Ping Kwan Tam for a useful discussion.

[1]H. F. Olson, "Gradient microphone," J. Acoust. Soc. Am. **17**(3), 192–198 (1946).
[2]B. R. Beavers and R. Brown, "Third-order gradient microphone for speech reception," J. Audio Eng. Soc. **16**(2), 636–640 (1970).
[3]G. M. Sessler and J. E. West, "Second-order gradient unidirectional microphones utilizing an electret transducer," J. Acoust. Soc. Am. **58**(1), 273–278 (1975).
[4]Y. Ishigaki, M. Yamamoto, K. Totsuka, and N. Miyaji, "Zoom microphon," in *Audio Engineering Society Convention* (1980), p. 1713.
[5]A. J. Brouns, "Second-order gradient noise-cancelling microphone," in *IEEE International Conference on Acoustics, Speech, and Signal Processing* (1981), pp. 786–789.
[6]G. S. Kang and D. A. Heide, "Acoustic noise reduction for speech communication (second-order gradient microphone)," in *IEEE International Symposium on Circuits and Systems*, Orlando, FL (30 May–2 June 1999), Vol. 4, pp. 556–559.
[7]P. C. Hines, A. L. Rosenfeld, B. H. Maranda, and D. L. Hutt, "Evaluation of the endfire response of a superdirective line array in simulated ambient noise environments," in *IEEE Oceans Conference*, Providence, RI (11–14 September 2000), Vol. 3, pp. 1489–1492.
[8]R. Aubauer and D. Leckschat, "Optimized second-order gradient microphone for hands-free speech recordings in cars," Speech Commun. **34**(1-2), 13–23 (2001).
[9]B. A. Cray, V. M. Evora, and A. H. Nuttall, "Highly directional acoustic receivers," J. Acoust. Soc. Am. **113**, 1526–1533 (2003).
[10]D. J. Schmidlin, "Directionality of generalized acoustic sensors of arbitrary order," J. Acoust. Soc. Am. **121**(6), 3569–3578 (2007).
[11]H. Cox and H. Lai, "Performance of line arrays of vector and higher order sensors," in *Asilomar Conference on Signals, Systems and Computers*, Pacific Grove, CA (4–7 November 2007), pp. 1231–1236.
[12]D. Kasilingam, D. Schmidlin, and P. Pacheco, "Super-resolution processing technique for vector sensors," in *IEEE Radar Conference*, Pasadena, CA (4–8 May 2009), pp. 1–4.
[13]Y. Song and K. T. Wong, "Closed-form direction finding using collocated but orthogonally oriented higher-order acoustic sensors," IEEE Sens. J. **12**(8), 2604–2608 (2012).
[14]H. F. Olson, *Acoustical Engineering*, 2nd ed. (D. Van Nostrand, Princeton, NJ, 1957).
[15]Y. Huang and J. Benesty, *Audio Signal Processing for Next-Generation Multimedia Communication Systems* (Kluwer Academic Publishers, New York, 2004).
[16]J. Benesty and J. Chen, *Study and Design of Differential Microphone Arrays* (Springer, Heidelberg, Germany, 2013).
[17]A. Nehorai and E. Paldi, "Acoustic vector-sensor array processing," IEEE Trans. Signal Process. **42**(10), 2481–2491 (1994).
[18]P. K. Tam and K. T. Wong, "Cramér-Rao bounds for direction finding by an acoustic vector-sensor under non-ideal gain-phase responses, non-collocation, or non-orthogonal orientation," IEEE Sens. J. **9**(8), 969–982 (2009).
[19]Y. I. Wu, K. T. Wong, and S.-K. Lau, "The acoustic vector-sensors near-field array-manifold," IEEE Trans. Signal Process. **58**(7), 3946–3951 (2010).
[20]The trigonometric functions' periods are unaffected by the power k. For example, $\sin(\gamma)$ and $\sin^k(\gamma)$ have the same period (other than due to any sign change for an even k). This kth power differs from $\sin(k\gamma)$, which would indeed change the period.
[21]B. D. V. Veen and K. M. Buckley, "Beamforming: A versatile approach to spatial filtering," IEEE Acoust., Speech, Signal Process. Mag. **5**(2), 4–24 (1988).
[22]K. T. Wong and H. Chi, "Beam patterns of an underwater acoustic vector hydrophone located away from any reflecting boundary," IEEE J. Ocean. Eng. **27**(3), 628–637 (2002).
[23]T.-C. Lin, K. T. Wong, M. O. Cordel, and J. P. Ilao, "Beamforming pointing error of a triaxial velocity sensor under gain uncertainties," J. Acoust. Soc. Am. **140**(3), 1675–1685 (2016).
[24]K. T. Wong, C. J. Nnonyelu, and Y. I. Wu, "A triad of cardioid sensors in orthogonal orientation and spatial collocation: its spatial-matched-filter-type beam-pattern," IEEE Trans. Signal Process. **66**(4), 895–906 (2018).
[25]C. J. Nnonyelu, "Pointing bias in 'spatial matched filter' beamforming at a tri-axial velocity-sensor due to non-perpendicular axes," World J. Innovative Res. **5**(2), 24–29 (2018).
[26]C. J. Nnonyelu, C. H. Lee, and K. T. Wong, "Directional pointing error in 'spatial matched filter' beamforming at a tri-axial velocity-sensor with non-orthogonal axes," in *Proceedings of Meetings on Acoustics*, Minneapolis, MN (7–11 May 2018), Vol. 33.
[27]Y. Song and K. T. Wong, "Beam patterns of a collocated pair/triad/quad of orthogonal acoustic sensors of 0th-/1st-/2nd-order directivity," in *Meeting of the Acoustical Society of America*, San Francisco, CA (2–6 December 2013).
[28]C. J. Nnonyelu, K. T. Wong, and C. H. Lee, "Higher-order figure-8 sensors in a pair, skewed and collocated-their 'spatial matched filter' beam-pattern," J. Acoust. Soc. Am. **147**(2), 1195–1206 (2020).
[29]C. J. Nnonyelu, Y. I. Wu, and K. T. Wong, "Cardioid microphones/hydrophones in a collocated and orthogonal triad: A steerable beamformer with no beam-pointing error," J. Acoust. Soc. Am. **145**(1), 575–588 (2019).